Inorganic Chemistry

Article

pubs.acs.org/IC

Nitric Oxide Release from a Nickel Nitrosyl Complex Induced by One-Electron Oxidation

Ashley M. Wright, Homaira T. Zaman, Guang Wu, and Trevor W. Hayton*

Department of Chemistry and Biochemistry, University of California—Santa Barbara, Santa Barbara, California 93106, United States

Supporting Information

ABSTRACT: Reaction of $[Ni(NO)(bipy)][PF_6]$ (**2**) with $AgPF_6$ or $[NO][PF_6]$ in MeCN results in formation of $[Ni(bipy)_x(MeCN)_y]^{2+}$ and release of NO gas in moderate yields. In contrast, the addition of the inner sphere oxidant Ph_2S_2 to **2** does not result in denitrosylation. Instead, the diphenyldisulfide adduct $[\{(bipy)(NO)Ni\}_2(\mu\text{-}S_2Ph_2)][PF_6]_2$ (**3**) is formed in good yield. However, oxidation of **2** with 2,2,6,6-tetramethylpiperidine-1-oxyl (TEMPO) does results in cleavage of the Ni−NO bond and generation of NO. The metal-containing product, $[(bipy)Ni(\eta^2\text{-TEMPO})][PF_6]$ (**4**), can be isolated as an orange-brown solid in excellent yields. In the solid state, complex **4** contains a side-on bound $TEMPO^-$ ligand, which is characterized by a long N−O bond length [1.383(2) Å]. The contrasting reactivity of Ph_2S_2 and TEMPO likely relates to their different redox potentials, as Ph_2S_2 is a relatively weak oxidant. Finally, the addition of pyridine-*N*-oxide to **2** results in the formation of the adduct, $[(bipy)Ni(NO)(ONC_5H_5)][PF_6]$ (**5**). No evidence of NO release is observed in this reaction, probably because of the low one-electron ($1e^-$) reduction potential of pyridine-*N*-oxide.

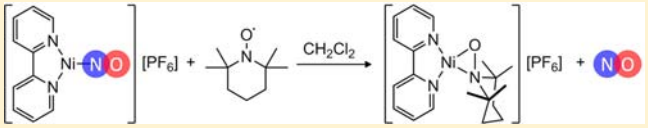

INTRODUCTION

The reactivity of nitric oxide (NO) remains a fundamentally important area of research. This is due in part to the extensive roles of NO in biology and in the environment.[1−9] Nitric oxide is an integral part of immune response, vasodilatation, and platelet aggregation,[5,10,11] and compounds that release NO have been sought for their potential use as therapeutics.[11−14] Several organic reagents, including alkyl nitrates (glyceryl trinitrate),[15] alkyl nitrites (iso-amyl nitrite),[5] and NONOates[16−18] have been utilized as NO-releasing compounds.[5,19] Metal nitrosyl complexes have also been used as NO delivery agents,[19] the classic example being sodium nitroprusside ($Na_2[FeNO(CN)_5]$, SNP).[20,21] Photodissociation,[12,13,22−25] reduction,[26] and oxidation[27−32] have all been employed to effect NO release from a metal nitrosyl complex. The latter two approaches, in particular, require a clear understanding of the redox chemistry of metal nitrosyl complexes. For instance, the mechanism of NO release from SNP is thought to involve an initial reduction event at the Fe center; however, this mechanism has not been fully elucidated.[5,33]

There are only a few well-defined examples of NO dissociation upon oxidation of a metal nitrosyl complex.[27−32] For instance, Bakac and co-workers reported that the one-electron ($1e^-$) oxidation of $[CrNO(H_2O)_5]^{2+}$ or $[L^1(H_2O)\text{-}CrNO]^{2+}$ (L^1 = 1,4,8,11-tetraazacyclotetradecane) resulted in rapid denitrosylation.[27−29] The putative $1e^-$ oxidation products ($[CrNOL_5]^{3+}$) were not detected, suggesting that denitrosylation occurred immediately upon electron transfer. Similarly, Ledgzins and co-workers investigated the reactivity of $[CpCr(NO)X_2]^-$ (X = Cl, Br, I, OTf) with a variety of oxidants.[34] They also observed that the nitrosyl ligand in the $\{CrNO\}^4$ oxidation product was unstable with respect to dissociation, except when X was a strong donor ligand, such as a dialkylamide.[35] Importantly, in both cases, a stable nitrosyl complex with an Enemark and Feltham notation of $\{CrNO\}^5$ is converted into an unstable $\{CrNO\}^4$ complex upon oxidation.[34−37] This suggests that further examples of oxidative denitrosylation could be discovered by exploiting the $\{MNO\}^{5/4}$ couple.[37] Another $\{MNO\}^{x/x-1}$ couple that may also be susceptible to oxidative denitrosylation is the $\{MNO\}^{10/9}$ couple. While there are relatively few examples of metal nitrosyls with an $\{MNO\}^{10}$ configuration,[38−44] the number of $\{MNO\}^9$ species is even smaller, suggesting that the latter configuration is particularly unstable. To our knowledge, there are only two examples of mono nitrosyls with a $\{MNO\}^9$ configuration,[45−47] namely, $Tp^{tBu,Me}Co(NO)$ (Tp = tris-pyrazolyl borate) and $[Co(NO)(np_3)][BPh_4]$ (np_3 = tris(2-diphenylphosphinoethyl)amine). Both compounds contain Co as the metal center and are supported by strongly donating tripodal scaffolds.[46,47] Furthermore, there are no $\{NiNO\}^9$ complexes in the literature. Therefore, we reasoned that oxidation of a $\{NiNO\}^{10}$ complex, to generate a $\{NiNO\}^9$ species, would likely result in denitrosylation. To this end, we have investigated the $1e^-$ oxidation of $[Ni(NO)(bipy)][PF_6]$, a $\{NiNO\}^{10}$ species, in an attempt to effect controlled NO release.

RESULTS AND DISCUSSION

Synthesis and Characterization of $[Ni(NO)(bipy)][PF_6]$. Addition of bipy to THF solutions of $Ni(NO)I(THF)_n$[48] results in the precipitation of (bipy)Ni(NO)(I) (**1**) as a green

Received: December 7, 2012
Published: February 22, 2013

   dx.doi.org/10.1021/ic302697v | Inorg. Chem. 2013, 52, 3207−3216

microcrystalline powder. Subsequent addition of 1.05 equiv of $AgPF_6$ to **1** in CH_2Cl_2 provides $[Ni(NO)(bipy)][PF_6]$ (**2**) in high yields (70%−80%) (Scheme 1). Complexes **1** and **2** have

Scheme 1

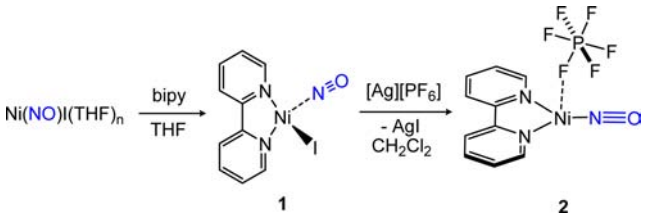

been characterized by X-ray crystallography, elemental analysis, and IR spectroscopy. Both complexes have been reported previously, but their characterization and solid-state structures have not been discussed.[39]

Complex **1** is sparingly soluble in THF and CH_2Cl_2, but is completely insoluble in nonpolar solvents, such as hexanes and diethyl ether. Its solution IR spectrum in CH_2Cl_2 exhibits a ν_{NO} stretch at 1792 cm^{-1}, while its ^1H NMR spectrum in CD_2Cl_2 contains three resonances at 7.76, 8.03, and 10.31 in a 2:4:2 ratio, assignable to aryl protons on the bipy ligand. Complex **1** crystallizes in the monoclinic space group $C2/m$ and its solid-state molecular structure is depicted in Figure 1. Complex **1**

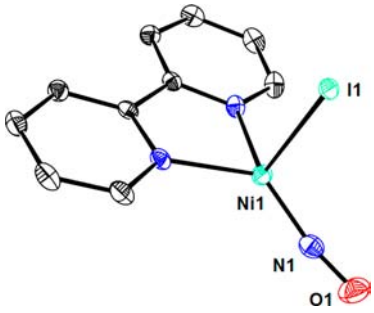

Figure 1. ORTEP drawing of (bipy)Ni(NO)(I) (**1**) shown with 50% thermal ellipsoids. Hydrogen atoms have been omitted for clarity. Selected bond lengths and bond angles: Ni1−N1 = 1.653(3) Å, N1−O1 = 1.153(4) Å, Ni2−I1 = 2.6013(4) Å, ∠N1−N1−O1 = 167.0(2)°.

features a severally distorted tetrahedral geometry about the Ni center (∠N2−N1−I1 = 99.74(5)°, ∠N1−Ni1−N2 = 132.30(6)°, ∠N1−Ni1−I1 = 105.12(9)°), a consequence of the small bite angle of the bipy ligand. In addition, the metrical parameters of the nitrosyl moiety (Ni1−N1 = 1.653(3) Å, N1−O1 = 1.153(4) Å, ∠Ni1−N1−O1 = 167.0(2)°) are consistent with other four-coordinated nickel nitrosyl complexes.[43]

Complex **2** is quite soluble in THF and CH_2Cl_2 but completely insoluble in nonpolar solvents, such as hexanes and diethyl ether. Its solution IR spectrum in CH_2Cl_2 exhibits a ν_{NO} value at 1869 cm^{-1}, which is toward the high end of values reported for other nickel nitrosyl complexes (range: 1568−1915 cm^{-1}).[38,40,43,49−52] The ^1H NMR spectrum of **2** in CD_2Cl_2 consists of four sharp resonances at 7.87, 7.95, 8.17, and 10.26 ppm, in a 2:2:2:2 ratio, which are assignable to the four proton environments of the bipy ligand. The ^{19}F and ^{31}P NMR spectra display significantly broadened resonances, at −72.4 ppm (full width at half maximum (fwhm) = 240 Hz) and −144.0 ppm (fwhm = 97 Hz), respectively. The broadening is ascribed to a weak dative interaction between the PF_6 anion and the electronically unsaturated Ni center. In accord with this hypothesis, the addition of a coordinating solvent, such as MeCN, results in a sharpening of these resonances, as formation of the solvento species, $[(bipy)Ni(NO)(NCMe)][PF_6]$, forces the PF_6 anion out of the Ni coordination sphere. The solution IR spectrum of the MeCN adduct exhibits an NO stretch at 1828 cm^{-1}, lower than that observed for **2** by 41 cm^{-1}.

Complex **2** crystallizes in the triclinic space group $P\bar{1}$ and its solid-state molecular structure is shown in Figure 2. There are

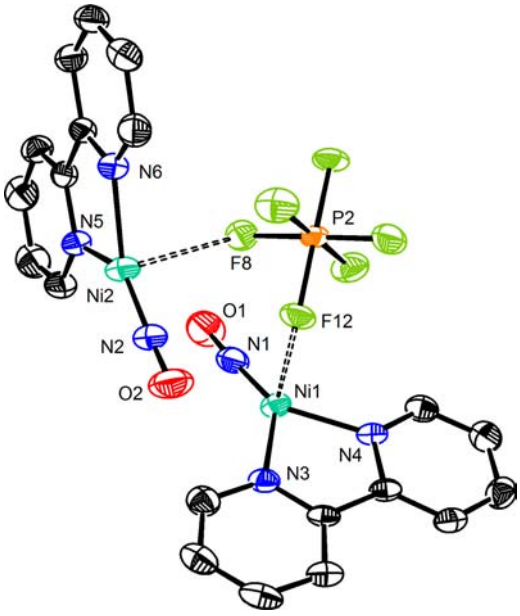

Figure 2. ORTEP drawing of $[Ni(NO)(bipy)][PF_6]$ (**2**) at 50% thermal ellipsoids. Hydrogen atoms and one PF_6 anion have been omitted for the sake of clarity. Selected bond lengths (Å) and bond angles (deg): Ni1−N1 = 1.617(3), N1−O1 = 1.152(4), Ni1−N3 = 1.976(3), Ni1−N4 = 1.963(2), Ni1···F12 = 2.697(2), ∠Ni1−N1−O2 = 176.2(3), Ni2−N2 = 1.611(3), N2−O2 = 1.153(4), Ni2−N5 = 1.970(3), Ni2−N6 = 1.956(3), Ni2···F8 = 2.947(2), ∠Ni2−N2−O2 = 174.7(3).

two independent nickel nitrosyl cations in the asymmetric cell. Each cationic Ni center is ligated by one bipy and one NO in an approximately trigonal planar environment. The metrical parameters of the Ni(NO) moieties are characterized by short Ni−N (1.617(3) Å; 1.611(3) Å) and N−O (1.152(4) Å; 1.153(4) Å) bond lengths and linear Ni−N−O bond angles (176.2(3)°; 174.7(3)°). Both independent $[Ni(NO)(bipy)]^+$ molecules exhibit long Ni···F contacts with a single PF_6 anion; however, the Ni−F distance varies considerably between the two molecules [Ni1−F12 = 2.697(2) Å; Ni2−F8 = 2.947(2) Å], and is likely quite weak in both instances. The second PF_6 anion does not interact with either Ni center. For comparison, the nickel complex $[Ni(L)_2(\eta^1\text{-F-}PF_5)][PF_6]$ (where L = 2-phenyl-1,4-bis(isopropyl)-1,4-diazabutadiene) contains a much shorter Ni···F contact of 2.453(2) Å.[53] Structurally characterized three coordinate nickel nitrosyls are quite rare.[50,54−56] For example, Storr and co-workers reported the neutral three coordinate nickel nitrosyl, $(\mu\text{-3,5-dimethylpyrazolyl-}N,N')_2(NiNO)_2$,[54] while Hillhouse and co-workers isolated the cationic $\{NiNO\}^{10}$ species, $[(dtbpe)Ni(NO)][BAr^F{}_4]$.[55] Not surprisingly, its Ni−N (Ni1−N1 =1.649(5) Å) and N−O (N−O = 1.141(8) Å) bond parameters are similar to those of **2**.

dx.doi.org/10.1021/ic302697v | Inorg. Chem. 2013, 52, 3207−3216

More recently, Warren and co-workers have reported the neutral three-coordinate nickel nitrosyls, [Ar_2nacnac]NiNO (Ar_2nacnac = Ar*N*C(Me)CHC(Me)*N*Ar; Ar = 2,6-^{i}Pr$_2$C$_6$H$_3$) and (IPr)NiNO(X) (IPr = *N*,*N*′-bis(2,6-diisopropylphenyl)-imidazole; X = I, OTf, SCPh$_3$).[50,56]

The electronic structure of nickel nitrosyl complexes has come under recent scrutiny.[45,57] Historically, nickel nitrosyl complexes were assigned a Ni^0(NO$^+$) electronic structure.[2] However, an extensive spectroscopic and theoretical study on Tp′M(NO) (where M = Co, Ni, Cu) suggested that, for the nickel analogue, the Ni^{II}(NO$^-$) electronic structure is the best description of its ground state. However, this description does not appear to be entirely adequate for complex **2**. For instance, its high NO stretching frequency [1868 cm^{-1}] and the short N−O bond length [1.152(4) Å vs 1.15 Å for NO gas] are more consistent with that expected for a Ni^I(NO$^•$) or Ni^0(NO$^+$) configuration. In addition, the related nickel nitrosyl, [Ni(NO)(bipy)$_2$][PF$_6$], which clearly exhibits a Ni^{II}(NO$^-$) electronic structure, features a much lower NO stretching frequency (1567 cm^{-1}) and substantially longer N−O bond length (1.207(3) Å).[39] Accordingly, we prefer the Ni^I(NO$^•$) or Ni^0(NO$^+$) configurations for complex **2**, as these better reflect its characterization data.

Cyclic Voltammetry of [Ni(NO)(bipy)][PF$_6$]. The solution phase redox properties of **2** were investigated by cyclic voltammetry. In MeCN at room temperature, the cyclic voltammogram of **2** displays an oxidation feature at +0.11 V (vs [Cp$_2$Fe]$^{0/+}$ at 100 mV/s) (see the Supporting Information (SI)), which is irreversible at all scan rates studied (up to 2 V/s). We propose that this feature reflects the formation of [Ni(NO)(bipy)]$^{2+}$, which is unstable and rapidly loses NO under the conditions of the experiment. Also observed in the cyclic voltammogram of **2** is a second irreversible oxidation feature at +0.90 V (vs [Cp$_2$Fe]$^{0/+}$ at 200 mV/s), which we have been unable to assign. No reduction features are observed within the solvent window at all scan rates. The cyclic voltammogram of **2** was also recorded in CH_2Cl_2; however, this trace is relatively complicated and consists of several indistinct oxidation features that we could not assign.

Oxidation of [Ni(NO)(bipy)][PF$_6$] with Outer Sphere Oxidants. With the electrochemical data for **2** in hand, we investigated its reactivity with a series of outer sphere oxidants. Gratifyingly, the one-electron (1e$^-$) oxidant AgPF$_6$ (0.65 V vs [Cp$_2$Fe]$^{0/+}$ in CH_2Cl_2; 0.04 V vs [Cp$_2$Fe]$^{0/+}$ in MeCN)[58] reacts with **1** in CH_2Cl_2 over the course of 2 h, resulting in the deposition of a silver mirror, the formation of a brown precipitate, and gas evolution (Scheme 2). The evolved gas was determined to be NO by gas chromatography−mass spectroscopy (GC/MS) and the yield was quantified to be 56% using a nitric oxide analyzer (NOA). Following this reaction via ^{1}H NMR spectroscopy in MeCN-d_3 reveals the formation of a mixture of paramagnetic products, tentatively formulated as [Ni(bipy)$_x$(CD$_3$CN)$_y$]$^{2+}$. The addition of 2 equiv of bipy to this reaction mixture results in complete conversion to [Ni(bipy)$_3$][PF$_6$]$_2$,[39] which can be isolated in 60% yield after workup. We also explored the reactivity of **2** with [NO][PF$_6$] (1.00 V vs [Cp$_2$Fe]$^{0/+}$ in CH_2Cl_2; 0.87 V vs [Cp$_2$Fe]$^{0/+}$ in MeCN).[58] The reaction of [NO][PF$_6$] with **2** in CH_2Cl_2/MeCN results in a rapid color change from dark blue to light purple, concomitant with gas evolution (see Scheme 2). An IR spectrum of the reaction mixture reveals the loss of the ν_{NO} stretch assignable to **2**. Moreover, N_2O was not observed in the IR spectrum, nor was the nitrosylation product of **2**, [(bipy)Ni(NO)$_2$][PF$_6$]$_2$.[39] Analysis of the head space by GC/MS reveals the presence of NO gas, and the yield of NO was determined to be 51% using the NOA (based on 2 equiv of NO being evolved during the reaction). Oxidation of **2** with [NO][PF$_6$] in MeCN, followed by the addition of 2 equiv of 2,2-bipyridine, also results in the formation of [Ni(bipy)$_3$][PF$_6$]$_2$, which can be isolated in 63% yield.[39] Importantly, the release of NO upon oxidation of **2** with either AgPF$_6$ or [NO][PF$_6$] confirms our initial hypothesis that the {MNO}$^{10/9}$ couple is susceptible to oxidative denitrosylation. Finally, we observed no reaction between **2** and [Cp$_2$Fe][PF$_6$] in CD_2Cl_2 over the course of 8 h. This is not surprising, given that the ferrocenium redox potential is lower than that of AgPF$_6$ or [NO][PF$_6$] in either MeCN or CH_2Cl_2.

Oxidation of [Ni(NO)(bipy)][PF$_6$] with Inner Sphere Oxidants. We also explored the reactivity of complex **2** with inner sphere oxidants, including disulfides, an important class of biological oxidants. Many sulfur-containing molecules, such as thiols and disulfides, are known to interact with nitric oxide.[59] For example, sulfhydryl-containing molecules, such as cysteine and glutathione, are thought to induce the release of NO from SNP upon reduction of the Fe center.[33] In contrast, disulfides are potential oxidants, and low-valent Group 10 metal complexes have been shown to induce disulfide bond cleavage.[60,61] With this in mind, we investigated the reactivity of diphenyl disulfide (Ph_2S_2) with **2**. Thus, the addition of 1 equiv of Ph_2S_2 to **2** at room temperature in CH_2Cl_2 results in a color change from dark green to blue-green. The solution IR spectrum of the reaction mixture reveals two ν_{NO} values at 1832 cm^{-1} and 1868 cm^{-1}, in a 1:4 ratio. The former stretch is assignable to [{(bipy)(NO)Ni}$_2$(μ-S_2Ph_2)][PF$_6$]$_2$ (**3**), whereas the latter stretch is assignable to unreacted **2**. The reaction equilibrium can be shifted completely to the product side, according to IR spectroscopy, via the addition of 15 equiv of Ph_2S_2 to solutions of **2** in CH_2Cl_2. However, complex **3** can be cleanly isolated on preparative scale in 59% yield as a blue crystalline material by addition of only 2.3 equiv of Ph_2S_2 to a CH_2Cl_2 solution of **2** (Scheme 3).

The formulation of **3** was established by X-ray diffraction (XRD) analysis of a blue block grown by slow diffusion of hexanes into a concentrated CH_2Cl_2 solution of **3** at −25 °C. Complex **3** crystallizes in the triclinic space group $P\bar{1}$, and its solid-state molecular structure is shown in Figure 3. The cation in complex **3** consists of a diphenyl disulfide ligand bridging two Ni metal centers. In addition, each nickel center is coordinated by a bipy ligand and a nitric oxide moiety in an overall distorted tetrahedral environment (e.g., ∠N3−Ni1−S1 = 111.90(11)°, ∠N3−Ni1−N1 = 130.90(14)°, ∠N3−Ni1−N2 = 129.76(14)°, τ_4 = 0.70).[62] The [NiNO]$^+$ moiety in **3** contains short Ni−N and N−O bond lengths [Ni1−N3 = 1.648(3) Å; N3−O1 = 1.153(4) Å], characteristic of cationic four-coordinated nickel nitrosyls.[2] The Ni−N−O bond angle

Scheme 2

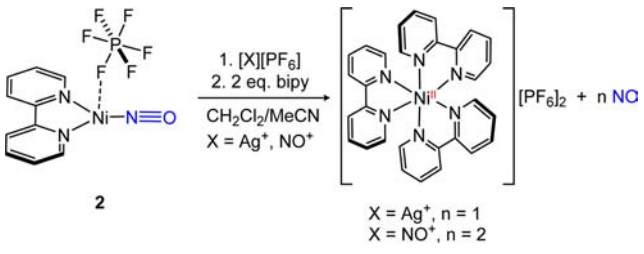

dx.doi.org/10.1021/ic302697v | Inorg. Chem. 2013, 52, 3207−3216

Scheme 3

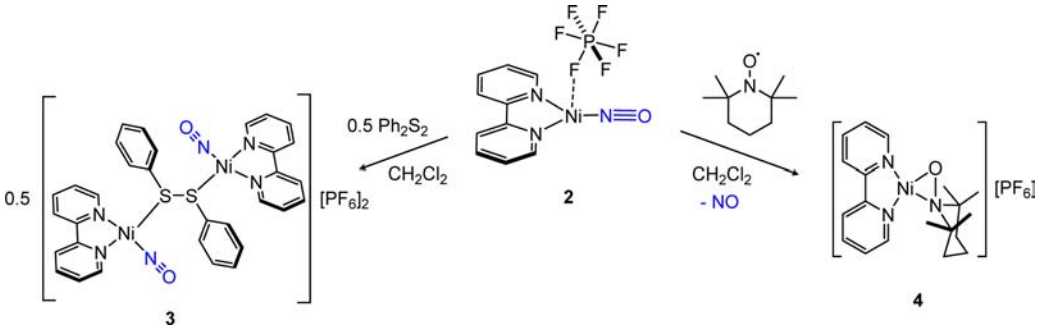

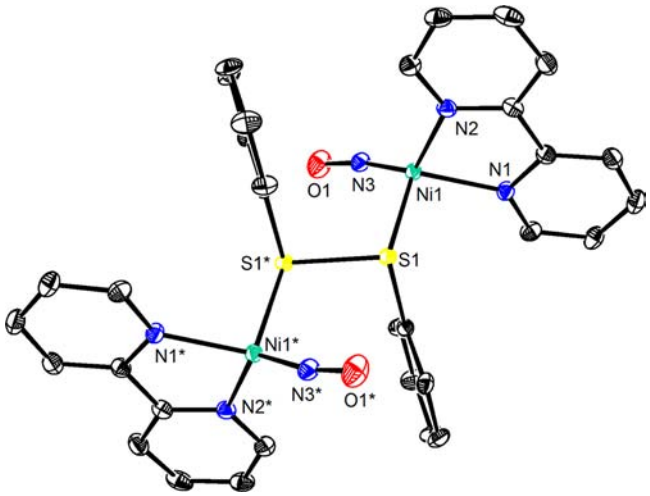

Figure 3. ORTEP drawing of $[\{Ni(NO)(bipy)\}_2(\mu\text{-}S_2Ph_2)][PF_6]_2$ ($\mathbf{3}\cdot 2CH_2Cl_2$) shown at 50% thermal ellipsoids. Hydrogen atoms, CH_2Cl_2 solvate, and PF_6 anions have been excluded for clarity. Selected bond lengths (Å) and bond angles (deg): Ni1−N1 = 1.648(3), N1−O3 = 1.153(4), Ni1−S1 = 2.3071(9), S1−S1* = 2.1306(17), Ni1−N1−O1 = 167.4(3).

(167.4(3)°) is slightly bent, the result of a non-C_3 symmetric ligand set.[63] The Ni−S bond length (2.3071(9) Å) is short, in comparison to other Ni−S dative bonds [2.42−2.55 Å]; however, in these examples, the sulfide donor is contained within a larger ligand scaffold that likely dictates the Ni−S bond distance. The S−S bond length in **3** (S1−S1* = 2.1306(17) Å) is elongated by 0.1 Å relative to free Ph_2S_2 (S−S = 2.03 Å).[64] To our knowledge, only two other complexes, $[ReBr(CO)_3]_2(Ph_2S_2)$ and $[Ag_2(Ph_2S_2)_4][AsF_6]_2$, exhibit a bridging disulfide similar to that found in **3**.[65]

The ^{1}H NMR spectrum of a crystalline sample of **3** in CD_2Cl_2 confirms the 2:1 ratio of Ni to Ph_2S_2 that was observed in the solid state. In addition, the ^{31}P and ^{19}F NMR spectra (CD_2Cl_2) feature broad PF_6^- signals, suggestive of a fluxional process involving displacement of the Ph_2S_2 ligand by PF_6^-. This is further evidenced by the solution IR spectrum (CH_2Cl_2) of isolated crystals of **3**, which exhibits two NO stretching values at 1868 cm^{-1} and 1832 cm^{-1}, assignable to **2** and **3**, respectively. The weak coordination of Ph_2S_2 to Ni is also apparent upon addition of a stronger donor ligand, such as MeCN, to a sample of **3** in CH_2Cl_2, which immediately generates $[(bipy)NiNO(MeCN)][PF_6]$ (ν_{NO} = 1828 cm^{-1}). Complex **3** is stable at room temperature for at least 24 h in CD_2Cl_2, according to ^{1}H NMR spectroscopy. Furthermore, thermolysis of **3** at 60 °C does not result in any apparent release of NO. Instead, complete decomposition of complex **3** is observed after 24 h, as determined by ^{1}H NMR spectroscopy, and no signals assignable to a paramagnetic Ni(II) complex were present in the spectrum (see Figure S37 in the SI). Nonetheless, it is clear that the addition of Ph_2S_2 to **2** does not result in oxidative denitrosylation under ambient conditions. This can be explained by examining its redox potential, as Ph_2S_2 is not an especially good oxidant (−2.00 V vs $[Cp_2Fe]^{+/0}$ in MeCN).[66,67] While coordination of Ph_2S_2 to a metal center is anticipated to change this potential, this effect is clearly not large enough to result in electron transfer from **2**.

We also explored the reactivity of **2** with TEMPO (TEMPO = 2,2,6,6-tetramethylpiperidine-1-oxyl). Like Ph_2S_2, TEMPO is also weak oxidant (−1.99 V vs $[Cp_2Fe]^{+/0}$ in MeCN), but its oxidation potential can be modulated greatly by coordination to a Lewis acid.[68] For example, $TEMPOH^+$ has a much higher oxidation potential (0.71 V vs $[Cp_2Fe]^{+/0}$ in MeCN) than free TEMPO.[67,69−71] Thus, the addition of TEMPO to a CH_2Cl_2 solution of **2** results in vigorous gas evolution and an immediate color change from dark green to orange. The IR spectrum of the reaction mixture reveals the loss of the ν_{NO} stretch for **2**. Furthermore, the appearance of a peak assignable to a new nitrosyl complex, or to N_2O, was not observed.[39] The evolved gas was identified as NO by GC/MS and the yield determined to be 59% using the NOA. In addition, monitoring the reaction by ^{1}H NMR spectroscopy reveals clean generation of a single metal-containing product. Crystallization from CH_2Cl_2/hexanes yields the diamagnetic Ni(II) complex, $[(bipy)Ni(\eta^2\text{-}TEMPO)][PF_6]$ (**4**), as a yellow-orange crystalline solid in 88% yield (see Scheme 3).

The composition of **4** was established by XRD analysis of a crystal grown from a dilute CH_2Cl_2/hexanes solution. Complex **4** crystallizes in the monoclinic space group $C2/c$, and the cationic portion of the molecule is shown in Figure 4. The nickel center is ligated by a single bipy ligand and a η^2-O,N-bound TEMPO ligand, in an overall square planar geometry. The Ni1−O1 and Ni1−N1 bond distances are 1.804(2) and 1.898(2) Å, and are comparable to previously characterized $Ni(\eta^2\text{-}TEMPO)$ complexes.[72,73] The N1−O1 bond distance [1.383(2) Å] is consistent with the presence of a reduced $TEMPO^-$ ligand. For comparison, this distance is similar to those found in $Ni(\eta^2\text{-}TEMPO)_2$ [1.3850(10) Å] and (κ^1-*P*-dtpbe)NiCl(TEMPO) [1.385(2) Å], which also feature reduced $TEMPO^-$ ligands.[72,73] In contrast, the neutral TEMPO ligand in $CuBr_2(\eta^2\text{-}TEMPO)$, contains a much shorter N−O bond distance of 1.304(8) Å.[74] The Ni1−N2 and Ni1−N3 bond lengths are 1.896(2) and 1.881(2) Å, respectively, and are comparable with previously reported square planar nickel(II) bipyridine complexes.[39]

dx.doi.org/10.1021/ic302697v | Inorg. Chem. 2013, 52, 3207−3216

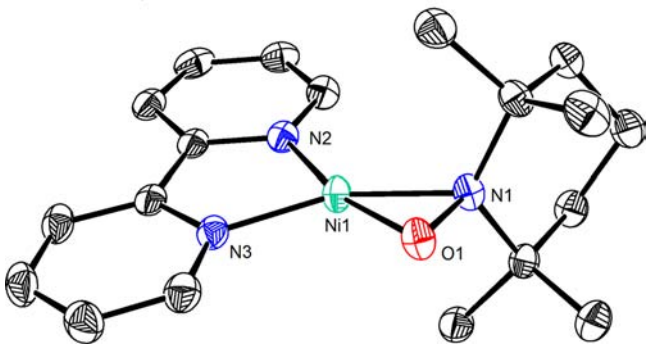

Figure 4. ORTEP drawing of $[Ni(bipy)(\eta^2\text{-TEMPO})][PF_6]$ ($\mathbf{4}\cdot 0.5CH_2Cl_2$) shown at 50% thermal ellipsoids. Hydrogen atoms, CH_2Cl_2 solvate, and PF_6 anion have been excluded for the sake of clarity. Selected bond lengths: Ni1−O1 = 1.804(2) Å, Ni1−N1 = 1.898(2) Å, N1−O1 =1.382(2) Å.

The ^{1}H NMR spectrum of **4** in CD_2Cl_2 exhibits two inequivalent methyl environments at 1.37 ppm and 2.60 ppm, which is consistent with the η^2 coordination mode observed in the solid state, and suggests the TEMPO coordination mode is static on the NMR time scale. In contrast, the ^{1}H NMR spectrum of $[Ni(\eta^2\text{-TEMPO})_2]$ exhibits broad spectral features, likely due to the fluxional coordination of the TEMPO ligand.[72] In addition, there are eight well-resolved bipy resonances in the aromatic region, also consistent with the η^2-TEMPO coordination mode. Finally, the ^{19}F and ^{31}P NMR spectra exhibit a doublet at −73.3 ppm (J_{FP} = 711 Hz) and a septet at −144.5 ppm (J_{PF} = 745 Hz), respectively, consistent with the presence of a PF_6 anion.

We propose that the reaction of **2** with TEMPO results in the formation of a transient {NiNO}^{9} intermediate, $[(bipy)Ni(NO)(\eta^1\text{-TEMPO})][PF_6]$ (Scheme 4). This species rapidly releases NO to generate the final product (**4**). As evidence, we note that the reaction of **2** with TEMPO in the presence of MeCN is substantially slower, suggesting that TEMPO must displace MeCN in the Ni-coordination sphere before oxidation can occur. The proposed inner sphere electron transfer is further evidenced by the lack of reactivity observed between TEMPO and the four-coordinated nitrosyl complex, (bipy)Ni(NO)(I) (**1**). As mentioned above, the redox potential of TEMPO can be greatly modulated by coordination to a Lewis acid.[68] Thus, while TEMPO is not a strong enough oxidant to effect the outer sphere oxidation of **2**, according to cyclic voltammetry, it is likely that upon binding to Ni, the redox potential of TEMPO is sufficiently shifted to induce electron transfer.

Scheme 4

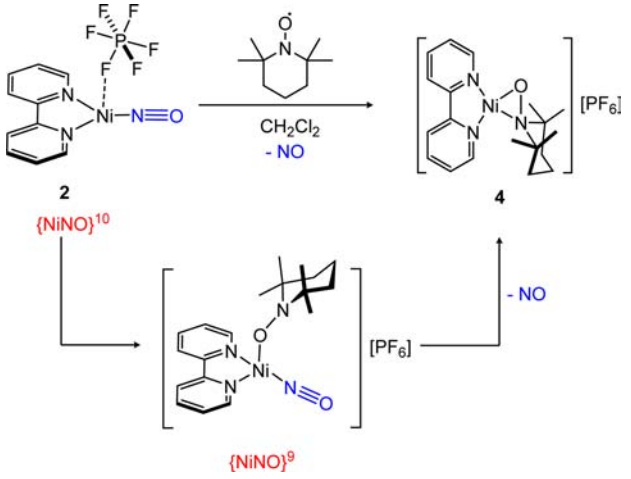

To evaluate the validity of the putative $[(bipy)Ni(NO)(\eta^1\text{-TEMPO})][PF_6]$ intermediate, we explored the reactivity of **2** with pyridine-*N*-oxide (C_5H_5NO). Previously, Drago and coworkers determined that the Lewis basicities of TEMPO and pyridine-*N*-oxide were comparable, as revealed by the heats of formation of their hydrogen-bonded adducts with phenol (TEMPO: $-\Delta H$ = 6.1 kcal/mol; C_5H_5NO: $-\Delta H$ = 8.1 kcal/mol).[75−77] However, the 1e$^-$ reduction potential of C_5H_5NO (−2.747 V vs $Cp_2Fe^{+/0}$ in DMF)[78] is much lower than that of TEMPO, making it less likely to induce oxidative denitrosylation by a 1e$^-$ oxidation event. Thus, treatment of a green CH_2Cl_2 solution of **2** with C_5H_5NO results in a rapid color change to deep blue. Crystallization from CH_2Cl_2/hexanes at −25 °C results in the isolation of $[(bipy)Ni(NO)(ONC_5H_5)][PF_6]$ (**5**) as a blue crystalline solid in 81% isolated yield (eq 1).

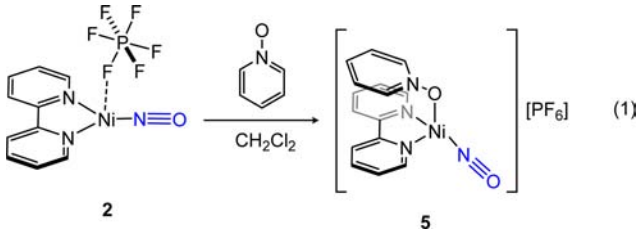

(1)

The observation that pyridine-*N*-oxide cannot effect oxidation denitrosylation of **2** is consistent with its low 1e$^-$ redox potential, while the lack of O-atom transfer to the NO ligand suggests a reasonably large kinetic barrier to N−O bond cleavage. In addition, the isolation of a stable pyridine-*N*-oxide adduct of the $[(bipy)Ni(NO)]^+$ fragment adds credence to the proposed mechanism of NO release described in Scheme 4.

The solid-state IR spectrum (Nujol mull) of **5** features a ν_{NO} stretch at 1801 cm^{-1}, which is among the lowest values yet observed for a cationic nickel nitrosyl,[39] demonstrating the strong donor ability of pyridine-*N*-oxide. Its ^{1}H NMR spectrum exhibits four well-defined resonances at 7.88, 8.06, 8.14, and 10.29 ppm, in a 2:2:2:2 ratio, assignable to the four bipy proton environments. In contrast, the resonances of the pyridine-*N*-oxide ligand, observed at 7.47, 7.61, and 8.26 ppm (2:1:2 ratio), are significantly broadened.[79] Moreover, the ^{19}F and ^{31}P NMR spectra of **5** feature a broadened doublet and septet, at −72.5 ppm (fwhm = 90 Hz) and −144.2 ppm (fwhm = 120 Hz), respectively. A plausible explanation for this phenomenon would be an equilibrium between **2** and **5**; however, this hypothesis is not supported by the solution IR spectrum in CH_2Cl_2, which features a single ν_{NO} stretch at 1817 cm^{-1}. While this is slightly higher than the NO stretch observed in Nujol, it is still much lower than the ν_{NO} stretch of **2** (1869 cm^{-1}). Furthermore, the deep blue color of **5** in CH_2Cl_2 suggests the presence of a four coordinate $[Ni(NO)L_3]^+$ species, as complexes of this type are typically blue.[43] Given these considerations, we suggest that there is a close-contact ion pair between the PF_6 anion and the Ni complex in solution, which restricts rotation of both the PF_6 moiety and the pyridine-*N*-oxide coligand, thereby explaining the broadened NMR signals.

dx.doi.org/10.1021/ic302697v | Inorg. Chem. 2013, 52, 3207−3216

The solid-state molecule structure of **5** has been determined by X-ray crystallography and the cationic portion of the molecule is shown in Figure 5. The cation in complex **5** consists

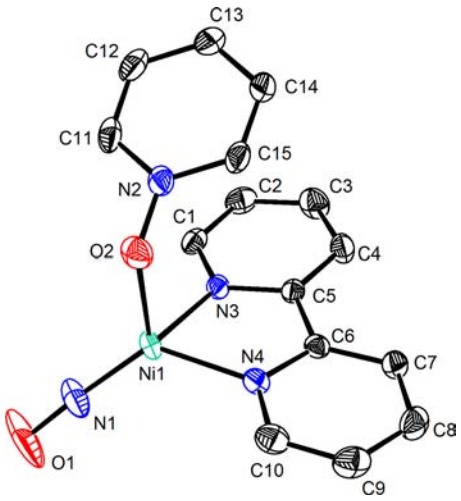

Figure 5. (a) ORTEP drawing of $[(bipy)Ni(NO)(ONC_5H_5)][PF_6]$ (**5**·0.5CH_2Cl_2) shown at 50% thermal ellipsoids. CH_2Cl_2 solvate, hydrogen atoms, and PF_6 anion have been excluded for the sake of clarity. Selected bond lengths (Å) and bond angles (deg): Ni1−N1 = 1.6300(18) Å, Ni1−O2 = 2.0323(15) Å, Ni1−N3 = 1.9983(16) Å, Ni1−N4 = 2.0084(17) Å, O1−N1 = 1.167(2) Å, O2−N2 = 1.337(2) Å; ∠Ni1−N1−O1 = 176.0(2)°.

of a Ni center ligated by a bipy ligand, an NO ligand, and an C_5H_5NO ligand, in an overall distorted tetrahedral geometry (τ_4 = 0.73).[62] The metrical parameters of the Ni−N−O moiety (Ni1−N1 = 1.6300(18) Å, N1−O1 = 1.167(2) Å; ∠Ni1−N1−O1 = 176.0(2)°) are characteristic of four-coordinated nickel nitrosyl complexes.[2,43,80,81] Furthermore, the Ni−O_{py} bond distance is 2.0323(15) Å and the N−O bond length of the C_5H_5NO ligand is 1.337(2) Å. For comparison, the N−O bond length in $[Ni(ONC_5H_5)_6][X]_2$ (X = BrO_3^- or BF_4^-) is 1.32 Å, while the N−O bond length for free pyridine-*N*-oxide is 1.330(9) Å, suggesting little activation of the N−O bond in **5**.[82−84]

CONCLUSIONS

One-electron ($1e^-$) oxidation of $[Ni(NO)(bipy)][PF_6]$ with $AgPF_6$, $[NO][PF_6]$, or TEMPO results in oxidative homolysis of the Ni−NO bond and subsequent evolution of NO gas, with NO yields ranging from 51 to 59%. In the case of the TEMPO reaction, the Ni oxidation product, $[(bipy)Ni(\eta^2\text{-TEMPO})][PF_6]$ can be isolated in 81% yield. Interestingly, the reaction of $[Ni(NO)(bipy)][PF_6]$ with Ph_2S_2 or pyridine-*N*-oxide does not lead to oxidative denitrosylation; instead, it results in the formation of the adducts $[\{Ni(NO)(bipy)\}_2(\mu\text{-}S_2Ph_2)][PF_6]_2$ and $[(bipy)Ni(NO)(ONC_5H_5)][PF_6]$, respectively. The lack of NO release in these examples can be rationalized by the low $1e^-$ reduction potentials observed for both diphenyl disulfide and pyridine-*N*-oxide. Overall, these results support our hypothesis that the $\{NiNO\}^9$ configuration is unstable, with respect to denitrosylation, and suggests that the $\{MNO\}^{10/9}$ couple could be harnessed in the design of a controlled NO release platform. This idea is further buttressed by the recent observation that dinitrosyliron complexes (DNICs) with a $\{Fe(NO)_2\}^9$ configuration are known to be more active toward NO loss than those with a $\{Fe(NO)_2\}^{10}$ configuration.[85,86]

EXPERIMENTAL SECTION

General. All reactions and subsequent manipulations were performed under anaerobic and anhydrous conditions under an atmosphere of nitrogen or argon. Nitromethane was recrystallized from Et_2O three times under a nitrogen atmosphere and then distilled over CaH_2; dichloromethane was degassed and stored over 3 Å sieves for 24 h before use. Diethyl ether, hexanes, and tetrahydrofuran (THF) were dried using a Vacuum Atmospheres DRI-SOLV solvent purification system. Deuterated NMR solvents (dichloromethane-d_2, 1,1,2,2-tetrachloroethane-d_2, nitromethane-d_3, acetonitrile-d_3) were dried over activated 3 Å molecular sieves for 24 h. $Ni(NO)I(THF)_n$ was prepared using previously published methods.[48] All other reagents were purchased from commercial suppliers and used as-received.

NMR spectra were recorded on a Varian UNITY INOVA 400 spectrometer or a Varian UNITY INOVA 500 spectrometer. The ^1H and ^{13}C NMR spectra were referenced to external $SiMe_4$, using the residual protio solvent peaks as an internal standard. The $^{19}F\{^1H\}$ NMR spectra were referenced to external $CFCl_3$ and $^{31}P\{^1H\}$ NMR spectra were referenced to external 85% phosphoric acid. IR spectra were recorded on a Thermo Scientific Nicolet 6700 FTIR spectrometer using NaCl plates for Nujol mulls or CaF_2 plates for solution-phase experiments. UV-vis experiments were performed with an Ocean Optics USB4000 UV-vis spectrometer equipped with a USB-DT light source or using a Shimadzu dual-beam Model UV-2401 PC spectrophotometer. Elemental analyses were performed by the Micro-Mass Facility at the University of California, Berkeley.

Gas Chromatography. Gas chromatography (GC) experiments were performed on an Agilent model 6890 gas chromatograph equipped with a thermal conductivity detector. The constituent gases were separated by passage through a 10-ft Carbosieve packed column using helium as the carrier gas. A typical experiment used the following procedure: the reaction components were loaded into a gas-tight piece of glassware and outfitted with a rubber septum in a glovebox. The reaction flask was stored inside the glovebox until the reaction was completed. The headspace was then sampled using a gas-tight syringe.

Cyclic Voltammetry Measurements. Cyclic voltammetry (CV) experiments were performed using a CH Instruments Model 600c potentiostat, and the data were processed using CHI software (Version 6.29). All experiments were performed in a glovebox using a 20-mL glass vial as the cell. The working electrode consisted of a platinum disk embedded in glass (2 mm in diameter), and both the counter and reference electrodes consisted of platinum wire. Solutions employed during the CV study were 1 mM in the nickel complex and 0.1 M in $[Bu_4N][PF_6]$. All potentials are reported versus the $[Cp_2Fe]^{0/+}$ couple. For all trials, $i_{p,a}/i_{p,c}$ = 1 for the $[Cp_2Fe]^{0/+}$ couple, while $i_{p,c}$ increased linearly with the square root of the scan rate (i.e., $v^{1/2}$).

Nitric Oxide Analyzer. Nitrogen monoxide was detected using a GE Nitric Oxide Analyzer (model NOA-280i). The head space of a gas-tight reaction flask was sampled using a Hamiliton gas-tight syringe. The samples were injected into the manifold setup using helium as the flow gas. The NOA was calibrated by injection of standard $NaNO_2$ solutions from 5 μM to 100 μM into a potassium iodide solution in glacial acetic acid. Calculations determining the amount of NO present in the reaction mixtures were performed by assuming that no nitric oxide remained dissolved in solution.[87]

Ni(NO)I(bipy) (1). To a stirring solution of $Ni(NO)(I)(THF)_n$ (153 mg, 0.424 mmol) in THF (2 mL) was added an excess of 2,2-bipyridine (72 mg, 0.46 mmol) in THF (1 mL). Immediately, a green microcrystalline precipitate formed. After stirring for 30 min, the product was collected on a medium porosity frit and washed with Et_2O (3 × 5 mL). 110 mg, 69% yield. Anal. Calcd. for $C_{10}H_8IN_3NiO$: C, 32.30; H, 2.17; N, 11.30. Found: C, 32.48; H, 2.24; N, 11.19. ^1H NMR (CD_2Cl_2, 22 °C, 400 MHz): δ 7.76 (m, 2H), 8.03 (m, 4H), 10.31 (d, 2H, J_{HH} = 4 Hz). IR (CH_2Cl_2 solution, cm^{-1}): 1792 (s, ν_{NO}). IR (Nujol mull, cm^{-1}): 1764 (s, ν_{NO}).

[Ni(NO)(bipy)][PF$_6$] (2). A CH_2Cl_2 (3 mL) suspension of $[Ag][PF_6]$ (195 mg, 0.77 mmol) was added to a stirring suspension of $[Ni(I)NO(bipy)]$ (280 mg, 0.75 mmol) in CH_2Cl_2 (5 mL). The mixture was stirred for 30 min, during which time the solution

dx.doi.org/10.1021/ic302697v | Inorg. Chem. 2013, 52, 3207−3216

changed to a dark green color, concomitant with precipitation of a flocculent white solid (AgI). The solution was filtered through a Celite column (2 cm × 0.5 cm) supported on glass wool, concentrated under reduced pressure, and layered with hexanes (3 mL). Subsequent storage at −25 °C for 24 h resulted in the deposition of dark green crystals. The supernatant was decanted and the crystals were washed with hexanes (1 × 3 mL) and dried in vacuo. 253 mg, 86% yield. Anal. Calcd. for $C_{10}H_8F_6N_3NiOP$: C, 30.81; H, 2.07; N, 10.78. Found: C, 31.13; H, 1.70; N, 10.47. ^{1}H NMR (CD_2Cl_2, 22 °C, 500 MHz): δ 7.87 (d, 2H, J_{HH} = 8 Hz) 7.95 (m, 2H) 8.17 (t of d, 2H, J_{HH} = 7.5 Hz and J_{HH} = 1 Hz) 10.26 (d, 2H, J_{HH} = 5 Hz). ^{1}H NMR (CD_3NO_2, 22 °C, 400 MHz): δ 8.00 (m, 2H) 8.20 (d, 2H, J_{HH} = 8 Hz) 8.25 (t of d, 2H, J_{HH} = 8 Hz and J_{HH} = 4 Hz) 10.41 (d, 2H, J_{HH} = 4 Hz). ^{19}F{^{1}H} NMR (CD_2Cl_2, 22 °C, 470 MHz): δ −72.42 (br d, PF_6^-, J_{PF} = 724 Hz). ^{31}P NMR (CD_2Cl_2, 22 °C, 202 MHz): δ −144.0 (br sept, PF_6^-, J_{PF} = 715 Hz). ^{13}C{^{1}H} NMR (CD_2Cl_2, 22 °C, 125 MHz): δ 121.88, 128.44, 142.48, 151.43. 153.19. IR (CH_2Cl_2 solution, cm^{-1}): 1869 (s, ν_{NO}). IR (Nujol mull, cm^{-1}): 1871 (s, ν_{NO}). UV−vis (CH_2Cl_2, 1.34 mM, 25 °C): 407 nm (ε = 225 L mol^{-1} cm^{-1}), 670 nm (ε = 291 L mol^{-1} cm^{-1}).

Oxidation of 2 with [Ag][PF$_6$]. *NMR spectroscopy.* An NMR tube was charged with [Ni(NO)(bipy)][PF$_6$] (34 mg, 0.088 mmol) and CD_2Cl_2 (0.5 mL), and an initial NMR spectrum was recorded. $AgPF_6$ (23 mg, 0.093 mmol) was then added as a CD_2Cl_2 suspension (0.5 mL). The reaction was monitored by ^{1}H NMR spectroscopy. After 24 h, a large amount of precipitate had deposited in the NMR tube. In addition, a silver mirror had formed on the walls of the NMR tube (see Figure S31 in the SI).

Nitric Oxide Analyzer. A stock solution of [Ni(NO)(bipy)][PF$_6$] in CH_2Cl_2 was prepared with a concentration of 5.15 mM. An aliquot of [Ni(NO)(bipy)][PF$_6$] (1.00 mL, 5.15 × 10^{-6} mol) was transferred using a syringe to a gas-tight reaction flask. Subsequently, $AgPF_6$ (1.6 mg, 6.3 × 10^{-6} mol), added as a suspension in CH_2Cl_2 (0.3 mL), was transferred to the reaction flask. Over the course of 3 h at room temperature, the reaction mixture faded from an intense green color to a light green color, concomitant with formation of a precipitate. A volume of 10 μL in the head space was sampled using a gas-tight syringe and injected into the NOA. The area of the resulting peak was compared to a calibration curve, and the amount of NO formation was determined to be 56% (average based on three injections).

Preparative Scale. A 20-mL scintillation vial was charged with [Ni(NO)(bipy)][PF$_6$] (83 mg, 0.212 mmol) and MeCN (2 mL). $AgPF_6$ (65 mg, 0.260 mmol) was added to the solution and the reaction mixture was stirred at room temperature. Over the course of 2 h, the solution changed from an intense purple to blue, concomitant with the formation of a brown precipitate. The solution was filtered through a Celite column (2 cm × 1 cm) supported on glass wool into a new scintillation vial containing bipy (76 mg, 0.49 mmol, 2.3 equiv), whereupon the solution became dark orange. The supernatant was layered with Et_2O (5 mL) and stored at −25 °C for 24 h, resulting in the deposition of red crystals of [Ni(bipy)$_3$][PF$_6$]$_2$. 104 mg, 60% yield. This material was spectroscopically identical to an authentic sample of [Ni(bipy)$_3$][PF$_6$]$_2$.[39]

Oxidation of 2 with [NO][PF$_6$]. *IR Spectroscopy.* [NO][PF$_6$] was added to a stirred CH_2Cl_2 solution of [Ni(NO)(bipy)][PF$_6$] (16 mg, 0.042 mmol), to which acetonitrile (10 μL, 0.19 mmol, 4.5 equiv) had been added. The dark blue solution converted to light purple over the course of 20 min. The in situ IR spectrum of this solution revealed the complete loss of the NO stretch of **2**. In addition, no peaks were observed that could be assigned to either a new NO complex or to N_2O. IR (CH_2Cl_2, cm^{-1}): 2057 (w, ν_{CN}) (see Figure S29 in the SI).

Gas chromatography. A gas-tight reaction flask was charged with [Ni(NO)(bipy)][PF$_6$] (38 mg, 0.097 mmol) and MeCN (0.73 mL). To this solution was added an MeCN solution (0.42 mL) of [NO][PF$_6$] (19 mg, 0.097 mmol) via syringe. The deep blue solution turned pale purple and gas evolution was observed. After 5 min at room temperature, a volume of 300 μL in the head space was sampled, using a gas-tight syringe, and a gas chromatogram was recorded, revealing the presence of N_2 and NO. No other products were observed in the chromatogram (see Figure S28 in the SI).

Nitric Oxide Analyzer. Stock solutions of [Ni(NO)(bipy)][PF$_6$] and [NO][PF$_6$] in MeCN were prepared with concentrations of 3.22 mM and 17.9 mM, respectively. An aliquot of the [Ni(NO)(bipy)][PF$_6$] solution (0.50 mL, 1.6 × 10^{-6} mol) was transferred via syringe to a gas-tight reaction flask. Subsequently, [NO][PF$_6$] (0.10 mL, 1.8 × 10^{-6} mol) was injected through a rubber septum into the reaction flask. The solution color changed from deep blue to light purple with concomitant gas evolution. After 5 min at room temperature, a volume of 10 μL in the head space was sampled using a gas-tight syringe and injected into the NOA. The area of the peak was compared to a calibration curve and the amount of NO formation was determined to be 51% (based on the formation of 2 equiv of NO).

Preparative Scale. [NO][PF$_6$] (47 mg, 0.27 mmol) was added to a MeCN solution (2 mL) of [Ni(NO)(bipy)][PF$_6$] (90 mg, 0.23 mmol). Gas evolution was observed immediately upon the addition, and the reaction color changed from deep purple to light purple. The reaction mixture was stirred for a total of 30 min, whereupon 2,2-bipyridine (87 mg, 0.55 mmol, 2.4 equiv) was added to the reaction mixture. The solution was filtered through a Celite column (2 cm × 1 cm) supported on glass wool and then reduced in vacuo to 1.5 mL. The solution was layered with Et_2O (5 mL) and subsequent storage at −25 °C for 6 h resulted in the deposition of a red-purple microcrystalline powder of [Ni(bipy)$_3$][PF$_6$]$_2$. 119 mg, 63% yield. ^{1}H NMR (CD_3CN, 22 °C, 400 MHz): δ 14.6 (br s, 12H), 46.3 (br s, 6H), 63.3 (br s, 6H). This material was spectroscopically identical to an authentic sample of [Ni(bipy)$_3$][PF$_6$]$_2$.[39]

[{(NO)(bipy)Ni}$_2$(μ-S$_2$Ph$_2$)][PF$_6$]$_2$ (3). A CH_2Cl_2 solution (1 mL) of [Ni(NO)(bipy)][PF$_6$] (71 mg, 0.18 mmol) was treated with a CH_2Cl_2 solution (1 mL) of diphenyl disulfide (91 mg, 0.42 mmol). The solution transformed from a green color to a dark blue color. The solution was subsequently layered with hexanes (5 mL), and storage at −25 °C for 24 h resulted in the deposition of blue blocks. 80 mg, 88% yield. Anal. Calcd for $C_{32}H_{26}F_{12}N_6Ni_2O_2P_2S_2$: C, 38.51; H, 2.63; N, 8.42. Found: C, 38.16; H, 2.75; N, 8.06. ^{1}H NMR (CD_2Cl_2, 22 °C, 400 MHz): δ 7.18−7.30 (m, 10H, Ph), 7.88 (dd, 4H, bipy, J_{HH} = 5.6 and 7.2 Hz), 7.92 (d, 4H bipy, J_{HH} = 8.4 Hz), 8.14 (t, 4H bipy, J_{HH} = 8 Hz), 10.06 (d, 4H bipy, J_{HH} = 8.4 Hz). ^{19}F NMR (CD_2Cl_2, 22 °C, 376 MHz): δ −66.21 (br s). ^{31}P NMR (CD_2Cl_2, 22 °C, 170 MHz): δ −140.1 (v br). IR (CH_2Cl_2, cm^{-1}): 1832 (ν_{NO}, s). IR (Nujol mull, cm^{-1}): 1836 (ν_{NO}, s).

[Ni(bipy)(η^2-TEMPO)][PF$_6$] (4). A CH_2Cl_2 (1 mL) solution of TEMPO (27 mg, 0.17 mmol) was added dropwise to a stirring solution of [Ni(NO)(bipy)][PF$_6$] (48 mg, 0.12 mmol) in CH_2Cl_2 (2 mL). Upon addition, the solution color changed from green to bright orange, with concomitant gas evolution. After 5 min of stirring, the solution volume was reduced in vacuo to 1.5 mL and filtered through a Celite column (0.5 cm × 0.5 cm) supported on glass wool. Addition of hexanes (4 mL) to the supernatant, followed by storage at −25 °C for 24 h, resulted in the precipitation of orange-yellow crystalline material. 52 mg, 81% yield. Anal. Calcd for $C_{19}H_{26}F_6N_3NiOP{\cdot}CH_2Cl_2$: C, 39.97; H, 4.70; N, 6.99. Found: C, 40.13; H, 4.83; N, 6.97. ^{1}H NMR (CD_2Cl_2, 400 MHz, 22 °C): δ 1.37 (s, 6H, Me), 1.58−1.99 (m 6H, CH_2), 2.60 (s, 6H, Me), 7.54 (m, 1H, bipy), 7.61 (m, 1H, bipy), 8.04 (d, 1H, J_{HH} = 8 Hz, bipy), 8.11 (d, 1H, 4 Hz, bipy), 8.13 (d, 1H, J_{HH} = 4 Hz, bipy), 8.16−8.22 (m, 2H, bipy), 8.36 (d, 1H, 8 Hz, bipy). ^{31}P{^{1}H} NMR (CD_2Cl_2, 170 MHz, 22 °C): δ −144.3 (sept, PF_6, J_{PF} = 745 Hz). ^{19}F NMR (CD_2Cl_2, 376 MHz, 22 °C): δ −73.3 (d, PF_6, J_{PF} = 711 Hz). ^{13}C NMR (CD_2Cl_2, 125 MHz, 22 °C): δ 16.69 (Me), 23.82 (Me), 34.09 (γ-CH_2 TEMPO), 39.38 (β-CH_2 TEMPO), 67.20 (α-C TEMPO), 122.82 (aryl H bipy), 123.19 (aryl H bipy), 127.86 (aryl H bipy), 128.84 (aryl H bipy), 141.16 (aryl H bipy), 141.32 (aryl H bipy), 151.42 (aryl H bipy), 153.35 (aryl H bipy), 154.17 (aryl H bipy), 154.51 (aryl H bipy). IR (Nujol mull, cm^{-1}): 1607 (w), 1460 (w), 1378 (m), 1315 (w), 1273 (w), 1250 (w), 1219 (w), 1169 (w), 1130 (w), 1076 (w), 1022 (w), 976 (w), 954 (w), 842 (s), 772 (m), 746 (w), 730 (m), 649 (w), 558 (w). UV-vis (0.45 mM, CH_2Cl_2, 25 °C): 394 nm (ε = 4400 L mol^{-1} cm^{-1}), 415 nm (ε = 3900 L mol^{-1} cm^{-1}), 464 nm (sh, ε = 1400 L mol^{-1} cm^{-1}).

[(bipy)Ni(NO)(ONC$_5$H$_5$)][PF$_6$] (5). A CH_2Cl_2 solution (1 mL) of pyridine-*N*-oxide (17 mg, 0.18 mmol) was added to a stirred CH_2Cl_2

dx.doi.org/10.1021/ic302697v | Inorg. Chem. 2013, 52, 3207−3216

Table 1. X-ray Crystallographic Data for Complexes 1−5

	1	2	3·2CH_2Cl_2	4·0.5CH_2Cl_2	5·0.5CH_2Cl_2
empirical formula	$C_{10}H_8IN_3NiO$	$C_{10}H_8F_6N_3NiOP$	$C_{34}H_{30}Cl_4F_{12}N_6Ni_2O_2P_2S_2$	$C_{19.50}H_{27}ClF_6N_3NiOP$	$C_{15.50}H_{14}ClF_6N_4NiO_2P$
crystal habit, color	block, green	rod, green	brick, dark blue	needle, yellow	block, blue
crystal size (mm)	0.25 × 0.20 × 0.18	0.60 × 0.20 × 0.02	0.20 × 0.20 × 0.03	0.20 × 0.05 × 0.05	0.30 × 0.15 × 0.15
crystal system	monoclinic	triclinic	triclinic	monoclinic	monoclinic
space group	$C2/m$	$P\bar{1}$	$P\bar{1}$	$C2/c$	$C2/c$
vol (Å^3)	1181.73(13)	1358.35(8)	1107.76(5)	4703(3)	3994.1(6)
a (Å)	13.9792(9)	7.9403(3)	10.1213(3)	21.240(7)	17.7511(15)
b (Å)	11.8611(8)	10.4457(3)	10.6254(3)	9.737(3)	10.5069(9)
c (Å)	7.7282(5)	16.9595(6)	12.2737(3)	22.745(8)	21.4383(19)
α (deg)	90	81.625(2)	75.043(2)	90	90
β (deg)	112.748(4)	86.498(2)	66.164(2)	90.718(6)	92.663(2)
γ (deg)	91	77.562(2)	67.598(2)	90	90
Z	4	4	1	8	8
formula weight, fw (g mol^{-1})	371.80	389.87	1167.92	558.57	527.44
density (calcd) (Mg M^{-3})	2.090	1.906	1.751	1.578	1.754
abs coeff (mm^{-1})	4.235	3.933	1.349	1.071	1.261
F_{000}	712	776	586	2296	2120
total no. reflections	5461	4976	10462	33969	28805
unique reflections	1883	3382	4533	4815	4086
R_{int}	0.0257	0.046	0.0277	0.0471	0.0352
final R indices [$I > 2\sigma(I)$]	R_1 = 0.0199, wR_2 0.0442	R_1 = 0.0498, wR_2 = 0.1483	R_1 = 0.0450, wR_2 = 0.1256	R_1 = 0.0297, wR_2 = 0.0640	R_1 = 0.0288, wR_2 = 0.0587
largest diff peak and hole (e$^-$ Å^{-3})	0.848 and −0.608	0.602 and −0.516	1.164 and −1.412	0.356 and −0.278	0.760 and −0.424
goodness of fit, GOF	1.041	1.062	1.102	1.005	1.139

(2 mL) solution of [Ni(NO)(bipy)][PF_6] (50 mg, 0.13 mmol). Immediately, the solution changed from green to royal blue. After 15 min of stirring, the reaction mixture was filtered through a Celite column supported on glass wool (0.5 cm × 2 cm). The filtrate was concentrated under reduced pressure to 1 mL and then layered with hexanes (4 mL). Subsequent storage at −25 °C for 24 h resulted in the precipitation of blue crystalline needles. 51 mg, 81% yield. Anal. Calcd for $C_{15}H_{13}F_6N_4NiO_2P$: C, 37.15; H, 2.70; N, 11.55. Found: C, 36.85; H, 2.86; N, 11.20. ^{1}H NMR (CD_2Cl_2, 400 MHz, 22 °C): δ 7.47 (br s, pyridine 2H), 7.61 (br s, pyridine 1H), 7.88 (t, 2H, bipy, J_{HH} = 8 Hz), 8.06 (d, 2H, bipy, J_{HH} = 8 Hz), 8.14 (t, 2H, bipy, J_{HH} = 8 Hz), 8.26 (br s, 2H, pyridine), 10.29 (d, 2H, bipy, J_{HH} = 4 Hz). ^{13}C NMR (CD_2Cl_2, 125 Hz, 22 °C): δ 122.2 (aryl H bpy), 127.8 (aryl H bpy), 140.2 (aryl H bpy), 152.2 (aryl H bpy). 152.7 (aryl H bpy). At 22 °C, only signals attributable to the bipy ligand are observed. ^{31}P{^{1}H} NMR (CD_2Cl_2, 170 MHz, 22 °C): δ −144.2 (br sept, PF_6, J_{PF} = 755 Hz, fwhm = 90 Hz). ^{19}F NMR (CD_2Cl_2, 376 MHz, 22 °C): δ −72.5 (br d, PF_6, J_{PF} = 711 Hz, fwhm = 120 Hz). IR (CH_2Cl_2, cm^{-1}): 1817 (s, ν_{NO}). IR (Nujol mull, cm^{-1}): 1802 (m, ν_{NO}), 1603 (m), 1574 (w), 1491 (w), 1466 (s), 1377 (m), 1318 (w), 1250 (w), 1202 (m), 1178 (m), 1160 (m), 1104 (w), 1072 (w), 1045 (w), 1025 (m), 935 (w), 835 (s), 767 (s), 733 (m), 673 (m), 651 (w), 639 (w), 557 (w). UV-vis (0.35 mM, CH_2Cl_2, 25 °C): 618 nm (ε = 275 L mol^{-1} cm^{-1}).

X-ray Crystallography. Data for **2** were collected on a Bruker Proteum2 diffractometer equipped with a PLATINUM CCD detector using multilayer optics with a Cu Kα X-ray source (α = 1.4178 Å). The crystals were mounted on a cryoloop under Paratone-N oil, and all data were collected at 100(2) K using an Oxford nitrogen gas cryostream system. Data were collected using ω scans with 0.5° frame widths. Frame exposures of 5 and 20 s were used for low-angle and high-angle diffractions, respectively. Data collection and cell parameter determination were conducted using the SMART program.[88] Integration of the data frames and final cell parameter refinement were performed using SAINT software.[89] Absorption correction of the data was carried out using the multiscan method SADABS.[90] Subsequent calculations were carried out using SHELXTL.[91] Structure determination was done using direct methods and difference Fourier techniques. All hydrogen atom positions were idealized, and rode on the atom of attachment. Structure solution, refinement, graphics, and creation of publication materials were performed using SHELXTL.[91] A PF_6 anion in complex **2** was disordered over two orientations in a 51:49 ratio.

Data for **1**, **3**, **4**, and **5** were collected on a Bruker KAPPA APEX II diffractometer equipped with an APEX II CCD detector using a TRIUMPH monochromator with a Mo Kα X-ray source (α = 0.71073 Å). The crystals were mounted on a cryoloop under Paratone-N oil, and all data were collected at 100(2) K, using an Oxford nitrogen gas cryostream system. Data were collected using ω scans with 0.5° frame widths. The frame exposures were as follows: 10 s for **1**, 5 s for **3**, 10 s for **4**, and 15 s for **5**. Data collection and cell parameter determination were conducted using the SMART program.[88] Integration of the data frames and final cell parameter refinement were performed using SAINT software.[89] Absorption correction of the data was carried out using the multiscan method SADABS.[90] Subsequent calculations were carried out using SHELXTL.[91] Structure determination was done using direct or Patterson methods and difference Fourier techniques. All hydrogen atom positions were idealized, and rode on the atom of attachment. Structure solution, refinement, graphics, and creation of publication materials were performed using SHELXTL. The PF_6 anion in **4** exhibits rotational disorder and was modeled over two orientations in a 63:37 ratio. The CH_2Cl_2 solvate molecule in **5** exhibits positional disorder, the Cl atom was modeled over two positions in a 55:45 ratio.

A summary of the relevant crystallographic data for complexes **1**−**5** can be found in Table 1.

■ ASSOCIATED CONTENT

Ⓢ Supporting Information

Experimental procedures, crystallographic details (as CIF files) and spectral data for compounds **1**−**5**. This material is available free of charge via the Internet at http://pubs.acs.org.

■ AUTHOR INFORMATION

Corresponding Author

*E-mail: hayton@chem.ucsb.edu.

Notes

The authors declare no competing financial interest.

■ ACKNOWLEDGMENTS

We thank the University of California, Santa Barbara and the Alfred P. Sloan Foundation for financial support of this work. We also thank Prof. Peter Ford and Meredith Crisalli for assistance with NOA measurements.

■ REFERENCES

(1) Butler, A. R.; Williams, D. L. H. *Chem. Soc. Rev.* **1993**, *22*, 233.
(2) Hayton, T. W.; Sharp, W. B.; Legzdins, P. *Chem. Rev.* **2002**, *102*, 935.
(3) Wasser, I. M.; de Vries, S.; Moenne-Loccoz, P.; Schroder, I.; Karlin, K. D. *Chem. Rev.* **2002**, *102*, 1201.
(4) Averill, B. A. *Chem. Rev.* **1996**, *96*, 2951.
(5) Williams, D. L. H. *Nitrosation Reactions and the Chemistry of Nitric Oxide*; Elsevier: Amsterdam, 2004.
(6) Legzdins, P.; Richter-Addo, G. B. *Metal Nitrosyls*; Oxford University Press: New York, 1992.
(7) Ford, P. C.; Fernandez, B. O.; Lim, M. D. *Chem. Rev.* **2005**, *105*, 2439.
(8) Ford, P. C.; Lorkovic, I. M. *Chem. Rev.* **2002**, *102*, 993.
(9) Beckman, J. S.; Koppenol, W. H. *Am. J. Physiol. Cell Physiol.* **1996**, *271*, C1424.
(10) Fang, F. C. *Nitric Oxide and Infection*; Kluwer Academic Publishers: New York, 1999.
(11) Fukumura, D.; Kashiwagi, S.; Jain, R. K. *Nat. Rev. Cancer* **2006**, *6*, 521.
(12) Ford, P. C. *Acc. Chem. Res.* **2008**, *41*, 190.
(13) Ford, P. C.; Bourassa, J.; Miranda, K.; Lee, B.; Lorkovic, I.; Boggs, S.; Kudo, S.; Laverman, L. *Coord. Chem. Rev.* **1998**, *171*, 185.
(14) Burks, P. T.; Ford, P. C. *Dalton Trans.* **2012**, *41*, 13030.
(15) Salvemini, D.; Mollace, V.; Pistelli, A.; Anggard, E.; Vane, J. *Proc. Natl. Acad. Sci. U.S.A.* **1992**, *89*, 982.
(16) Hrabie, J. A.; Klose, J. R.; Wink, D. A.; Keefer, L. K. *J. Org. Chem.* **1993**, *58*, 1472.
(17) Keefer, L. K.; Nims, R. W.; Davies, K. M.; Wink, D. A. In *Methods in Enzymology*; Lester, P., Ed.; Academic Press: New York, 1996; Vol. *268*, p 281.
(18) Hrabie, J. A.; Keefer, L. K. *Chem. Rev.* **2002**, *102*, 1135.
(19) Wang, P. G.; Xian, M.; Tang, X.; Wu, X.; Wen, Z.; Cai, T.; Janczuk, A. J. *Chem. Rev.* **2002**, *102*, 1091.
(20) Swinehart, J. H. *Coord. Chem. Rev.* **1967**, *2*, 385.
(21) Butler, A. R.; Megson, I. L. *Chem. Rev.* **2002**, *102*, 1155.
(22) Merkle, A. C.; Fry, N. L.; Mascharak, P. K.; Lehnert, N. *Inorg. Chem.* **2011**, *50*, 12192.
(23) Eroy-Reveles, A. A.; Leung, Y.; Beavers, C. M.; Olmstead, M. M.; Mascharak, P. K. *J. Am. Chem. Soc.* **2008**, *130*, 4447.
(24) Rose, M. J.; Mascharak, P. K. *Coord. Chem. Rev.* **2008**, *252*, 2093.
(25) Castano, A. P.; Mroz, P.; Hamblin, M. R. *Nat. Rev. Cancer* **2006**, *6*, 535.
(26) Lang, D. R.; Davis, J. A.; Lopes, L. G. F.; Ferro, A. A.; Vasconcellos, L. C. G.; Franco, D. W.; Tfouni, E.; Wieraszko, A.; Clarke, M. J. *Inorg. Chem.* **2000**, *39*, 2294.
(27) Song, W.; Bakac, A. *Chem.—Eur. J.* **2008**, *14*, 4906.
(28) Kristian, K. E.; Song, W.; Ellern, A.; Guzei, I. A.; Bakac, A. *Inorg. Chem.* **2010**, *49*, 7182.
(29) Song, W.; Ellern, A.; Bakac, A. *Inorg. Chem.* **2008**, *47*, 8405.
(30) Herold, S. *Inorg. Chem.* **2004**, *43*, 3783.
(31) Herold, S.; Boccini, F. *Inorg. Chem.* **2006**, *45*, 6933.
(32) Boccini, F.; Domazou, A. S.; Herold, S. *J. Phys. Chem. A* **2006**, *110*, 3927.
(33) Grossi, L.; D'Angelo, S. *J. Med. Chem.* **2005**, *48*, 2622.
(34) Legzdins, P.; McNeil, W. S.; Rettig, S. J.; Smith, K. M. *J. Am. Chem. Soc.* **1997**, *119*, 3513.
(35) Smith, K. M.; McNeil, W. S.; Legzdins, P. *Chem.—Eur. J.* **2000**, *6*, 1525.
(36) Legzdins, P.; J. Rettig, S.; M. Smith, K.; Tong, V.; G. Young, V., Jr. *J. Chem. Soc., Dalton Trans.* **1997**, 3269.
(37) Legzdins, P.; McNeil, W. S.; Smith, K. M.; Poli, R. *Organometallics* **1998**, *17*, 615.
(38) Tennyson, A. G.; Dhar, S.; Lippard, S. J. *J. Am. Chem. Soc.* **2008**, *130*, 15087.
(39) Wright, A. M.; Wu, G.; Hayton, T. W. *J. Am. Chem. Soc.* **2012**, *134*, 9930.
(40) Del, Z. A.; Mezzetti, A.; Novelli, V.; Rigo, P.; Lanfranchi, M.; Tiripicchio, A. *J. Chem. Soc., Dalton Trans.* **1990**, 1035.
(41) Feltham, R. D. *J. Inorg. Nucl. Chem.* **1960**, *14*, 307.
(42) Green, J. C.; Underwood, C. *J. Organomet. Chem.* **1997**, *528*, 91.
(43) Wright, A. M.; Wu, G.; Hayton, T. W. *Inorg. Chem.* **2011**, *50*, 11746.
(44) Wright, A. M.; Wu, G.; Hayton, T. W. *J. Am. Chem. Soc.* **2010**, *132*, 14336.
(45) Tomson, N. C.; Crimmin, M. R.; Petrenko, T.; Rosebrugh, L. E.; Sproules, S.; Boyd, W. C.; Bergman, R. G.; DeBeer, S.; Toste, F. D.; Wieghardt, K. *J. Am. Chem. Soc.* **2011**, *133*, 18785.
(46) Thyagarajan, S.; Incarvito, C. D.; Rheingold, A. L.; Theopold, K. H. *Inorg. Chim. Acta* **2003**, *345*, 333.
(47) Di Vaira, M.; Ghilardi, C. A.; Sacconi, L. *Inorg. Chem.* **1976**, *15*, 1555.
(48) Haymore, B.; Feltham, R. D. *Inorg. Synth.* **1973**, *14*, 81.
(49) Feltham, R. D. *Inorg. Chem.* **1964**, *3*, 116.
(50) Varonka, M. S.; Warren, T. H. *Organometallics* **2010**, *29*, 717.
(51) Landry, V. K.; Parkin, G. *Polyhedron* **2007**, *26*, 4751.
(52) Fullmer, B. C.; Pink, M.; Fan, H.; Yang, X.; Baik, M.-H.; Caulton, K. G. *Inorg. Chem.* **2008**, *47*, 3888.
(53) Muresan, N.; Chlopek, K.; Weyhermüller, T.; Neese, F.; Wieghardt, K. *Inorg. Chem.* **2007**, *46*, 5327.
(54) Chong, K. S.; Rettig, S. J.; Storr, A.; Trotter, J. *Can. J. Chem.* **1979**, *57*, 3090.
(55) Iluc, V. M.; Miller, A. J. M.; Hillhouse, G. L. *Chem. Commun.* **2005**, 5091.
(56) Puiu, S. C.; Warren, T. H. *Organometallics* **2003**, *22*, 3974.
(57) Landry, V. K.; Pang, K.; Quan, S. M.; Parkin, G. *Dalton Trans.* **2007**, 820.
(58) Connelly, N. G.; Geiger, W. E. *Chem. Rev.* **1996**, *96*, 877.
(59) Gaston, B. *Biochim. Biophys. Acta, Bioenerg.* **1999**, *1411*, 323.
(60) Zanella, R.; Ros, R.; Grazian, M. *Inorg. Chem.* **1973**, *12*, 2736.
(61) Taniguchi, N. *J. Org. Chem.* **2004**, *69*, 6904.
(62) Yang, L.; Powell, D. R.; Houser, R. P. *Dalton Trans.* **2007**, 955.
(63) Enemark, J. H.; Feltham, R. D. *Coord. Chem. Rev.* **1974**, *13*, 339.
(64) Lee, J. D.; Bryant, M. W. R. *Acta Crystallogr. Sect. B: Struct. Crystallogr. Cryst. Chem.* **1969**, *25*, 2094.
(65) Roesky, H. W.; Gries, T.; Jones, P. G.; Weber, K.-L.; Sheldrick, G. M. *J. Chem. Soc., Dalton Trans.* **1984**, 1781.
(66) Borsari, M.; Cannio, M.; Gavioli, G. *Electroanalysis* **2003**, *15*, 1192.
(67) Pavlishchuk, V. V.; Addison, A. W. *Inorg. Chim. Acta* **2000**, *298*, 97.
(68) Scepaniak, J. J.; Wright, A. M.; Lewis, R. A.; Wu, G.; Hayton, T. W. *J. Am. Chem. Soc.* **2012**, *134*, 19350.
(69) Marx, L.; Schollhorn, B. *New J. Chem.* **2006**, *30*, 430.
(70) Warren, J. J.; Tronic, T. A.; Mayer, J. M. *Chem. Rev.* **2010**, *110*, 6961.
(71) Semmelhack, M. F.; Chou, C. S.; Cortes, D. A. *J. Am. Chem. Soc.* **1983**, *105*, 4492.
(72) Isrow, D.; Captain, B. *Inorg. Chem.* **2011**, *50*, 5864.
(73) Mindiola, D. J.; Waterman, R.; Jenkins, D. M.; Hillhouse, G. L. *Inorg. Chim. Acta* **2003**, *345*, 299.
(74) Caneschi, A.; Grand, A.; Laugier, J.; Rey, P.; Subra, R. *J. Am. Chem. Soc.* **1988**, *110*, 2307.
(75) Herlocker, D. W.; Drago, R. S.; Meek, V. I. *Inorg. Chem.* **1966**, *5*, 2009.
(76) Drago, R. S.; Lim, Y. Y. *J. Am. Chem. Soc.* **1971**, *93*, 891.
(77) Joesten, M. D.; Drago, R. S. *J. Am. Chem. Soc.* **1962**, *84*, 3817.

(78) Kubota, T.; Nishikida, K.; Miyazaki, H.; Iwatani, K.; Oishi, Y. *J. Am. Chem. Soc.* **1968**, *90*, 5080.
(79) Hong, S.; Gupta, A. K.; Tolman, W. B. *Inorg. Chem.* **2009**, *48*, 6323.
(80) Rigo, P. *Inorg. Chim. Acta* **1980**, *44*, L223.
(81) Berglund, D.; Meek, D. W. *Inorg. Chem.* **1972**, *11*, 1493.
(82) Paduan-Filho, A.; Sinn, E.; Chirico, R. D.; Carlin, R. L. *Inorg. Chem.* **1981**, *20*, 2688.
(83) van Ingen Schenau, A. D.; Verschoor, C. G.; Romers, C. *Acta Crystallogr., Sect. B: Struct. Crystallogr. Cryst. Chem.* **1974**, *30*, 1686.
(84) Marsh, R. E.; Kapon, M.; Hu, S.; Herbstein, F. H. *Acta Crystallogr., Sect. B: Struct. Sci.* **2002**, *58*, 62.
(85) Hess, J. L.; Hsieh, C.-H.; Reibenspies, J. H.; Darensbourg, M. Y. *Inorg. Chem.* **2011**, *50*, 8541.
(86) Tonzetich, Z. J.; Héroguel, F.; Do, L. H.; Lippard, S. J. *Inorg. Chem.* **2011**, *50*, 1570.
(87) *Oxides of Nitrogen, Solubility Data Series*; Pergamon Press: Oxford, U.K., 1981; Vol. *8*.
(88) *SMART Software Users Guide*, Version 5.1; Bruker Analytical X-ray Systems, Inc.: Madison, WI, 1999.
(89) *SAINT Software Users Guide*, Version 5.1; Bruker Analytical X-ray Systems, Inc.: Madison, WI, 1999.
(90) Sheldrick, G. M. *SADABS*; University of Göttingen: Göttingen, Germany, 2005.
(91) Sheldrick, G. M. *SHELXTL PC*, Version 6.12; Bruker Analytical X-ray Systems, Inc.: Madison, WI, 2006.